

Combined electrification and carbon capture for low-carbon cement: techno-economic assessment of different designs

Leonardo Varnier^{a,b}, Federico d'Amore^{a,*}, Kim Clausen^b, Georgios Melitos^{a,c}, Bart de Groot^c,
Fabrizio Bezzo^{a,*}

*a. CAPE-Lab – Computer-Aided Process Engineering Laboratory
Department of Industrial Engineering
University of Padova
Via Marzolo 9, 35131 Padova (Italy)*

*b. FLSmidth Cement A/S
Vigerslev Allé 77, 2500 Valby, Copenhagen (Denmark)*

*c. Siemens Industry Software Limited
Hammersmith Grove 26-28, W6 7HA London (United Kingdom)*

* To whom all correspondence should be addressed:
federico.damore@unipd.it (Federico d'Amore)
fabrizio.bezzo@unipd.it (Fabrizio Bezzo)

Abstract

The cement industry is a major contributor to global CO₂ emissions. Among the various decarbonisation strategies, heat demand electrification and carbon capture technologies offer promising solutions for reducing both process- and fuel-related emissions.

This study investigates the potential of low-carbon cement plants that combine calciner electrification with amine-based carbon capture on rotary kiln emissions. A techno-economic analysis is conducted on four process alternatives, differing in the type of electrified calciner – entrainment vs. drop tube – and the heat recovery strategy for the hot CO₂ produced, in the EU context. The four low-carbon processes are benchmarked against a reference plant without mitigation measures.

Drop tube calciner configurations show better energy efficiency than entrainment calciner alternatives although their environmental performance is comparable. When renewable electrical energy is supplied to the plants, the CO₂ avoidance rates exceed 98%, making these options competitive with other decarbonisation technologies such as oxyfuel and calcium looping.

Economic viability remains challenging under current EU prices and carbon intensity of imported electricity. The entrainment calciner configuration that uses pure CO₂ to preheat raw materials emerges as the most favourable, with a cost of avoided CO₂ of 217.4 €/t_{CO₂}, compared to 231-234 €/t_{CO₂} for the other options. To ensure cost-effectiveness, electricity prices would need to remain below approximately 90 €/MWh_{el} when low-carbon electricity is supplied.

Keywords: *cement production, decarbonisation, electrification, calciner, carbon capture, techno-economic assessment.*

1. Introduction

The cement industry is responsible for approximately 2.5 Gt of CO₂ emissions annually, primarily from clinker production, accounting for 7% of global emissions (Marmier, 2023). Cement is classified as a “hard-to-abate” sector because around 60% of its CO₂ emissions are process-related, originating from the calcination reaction of limestone (CaCO₃), which decomposes into lime (CaO) and CO₂. The remaining CO₂ emissions are generated by the combustion of fossil fuels, with coal being the primary fuel used in most industrial applications (Cavalett et al., 2024). Given these two major sources of CO₂ emissions, it is essential to explore various complementary mitigation approaches (Strunge et al., 2024). Existing measures include carbon capture and storage (CCS) (Hills et al., 2016; Plaza et al., 2020), electrification of the process heat demand (Madeddu et al., 2020), fossil fuel substitution with alternative fuels (Nhuchhen et al., 2021; Yang et al., 2021), and clinker substitution with supplementary cementitious materials (Miller et al., 2016).

CCS technologies are widely recognised as crucial for addressing the process-related emissions from cement plants (IEA, 2018; GCCA, 2021) and numerous studies have explored various techniques to abate such CO₂. The CEMCAP project (CEMCAP, 2015) assessed and benchmarked several technologies, including monoethanolamine (MEA) absorption, oxyfuel combustion, calcium looping, membrane-assisted CO₂ liquefaction and chilled ammonia. From these alternatives, oxyfuel and calcium looping emerged as promising technologies, encouraging further research in subsequent projects aimed at advancing their maturity (CLEANKER, 2017; AC2OCEM, 2019; Catch4Climate, 2020). The LEILAC project (LEILAC, 2016) investigated the potential for direct separation of process emissions through indirect heating of limestone in a drop tube (DT) calciner. This system enables to keep separated the flue gas from combustion and capturing the pure CO₂ from calcination. Pilot plant results demonstrated successful CO₂ separation without compromising the energy efficiency of the calciner, leading to continued development in the LEILAC2 project (LEILAC2, 2020).

While carbon capture remains essential for reducing process emissions, electrification of heat demand offers a promising solution to reduce fuel-related CO₂ emissions, which constitute about 40% of total direct emissions (Schneider et al., 2023). Cement production can be electrified through plasma technology, induction heating, resistive electrical heating and microwave heating (Antunes et al., 2022). However, only the direct electrification of the heat duty of the calciner appears a viable short-term solution. This unit operates at approximately 900°C, and technologies that supply heat below 1000°C are well-established and require minimal retrofitting (Madeddu et al., 2020). An electrified calciner offers two key advantages for a low-carbon cement plant: it removes the fuel-related CO₂ emissions and produces a pure CO₂ stream from the calcination reaction, ready for utilisation or storage.

In this context, Tokheim et al., (2019) assessed the technical and economic feasibility of a rotary calciner with resistance-based heating. Jacob and Tokheim, (2023) compared the energy demand of a cement plant using different electrified calciner designs, all employing a gas-gas heat exchanger for heat recovery from the pure CO₂ stream. They modelled various designs, including entrainment (Ent) calciner, fluidised bed calciner, and rotary calciner, with varying degrees of CO₂ recycling. Other studies by the same group concluded that a full-scale electrified rotary calciner is not recommended due to its required size, while electrifying an entrainment calciner with heating rods was found to be technically feasible (Jacob and Tokheim, 2021; Jacob et al., 2023).

Quevedo Parra and Romano (2023) compared the technical and economic performance of various configurations for partial or full electrification of a cement plant. Two alternatives involved an electrified DT-calciner using resistive elements, where they considered utilising the hot CO₂ stream to preheat the raw meal in a separate cyclone tower. In one scenario, MEA-based capture was used to address residual emissions from the kiln. A recent report from LEILAC2 (LEILAC2, 2023) also assessed the technical and economic feasibility of an electrified DT-calciner, confirming that this technology is being developed to operate on multiple energy sources, including electricity.

In summary, most research on cement sector decarbonisation has focused on evaluating carbon capture technologies and electrifying heat demand separately. Only few techno-economic studies explored the combination of calciner electrification with CO₂ abatement from the rotary kiln, with a primary focus on processes involving a DT-calciner, in which the hot CO₂ stream is used to preheat the raw meal (LEILAC2, 2023; Quevedo Parra and Romano, 2023). Moreover, there is a lack of economic analyses exploring alternative heat recovery methods for pure CO₂ or the electrification of an Ent-calciner. Consequently, the full potential of these approaches and the most effective implementation strategies remain unclear.

To address this gap, this study evaluates the techno-economic performance of different low-carbon cement processes that combine calciner electrification and amine-based capture applied to emissions from the rotary kiln, in the EU context. Specifically, four alternatives are designed, which differ in the type of electrified calciner – either Ent or DT – and the heat recovery strategy for the pure CO₂ stream exiting the calciner. The key contributions of this study are as follows:

- Comparing the low-carbon alternatives within a consistent framework of technical and economic assumptions (calciner temperature, calcination extent, equipment cost estimates, etc.), allowing for the identification of strengths, weaknesses, and trade-offs between the technologies.
- Evaluating the economic feasibility of low-carbon cement plants with an electrified Ent-calciner alongside alternative heat recovery strategies for pure CO₂ exiting the calciner.
- Employing response surface models that leverage data generated in-silico through Design of Experiments techniques to assess the sensitivity of economic performance to key parameters (e.g., electricity price, grid carbon intensity) so as to evaluate the combined effect of multiple factors.
- Adjusting the raw meal composition to account for variations in fuel ash in the low-carbon plants, which is overlooked in other studies and may lead to incorrect clinker chemistry.

The article is structured as follows. Section 2 details the methods for designing and modelling the reference cement plant and the low-carbon alternatives, along with the methodology for the economic assessment and the definition of key performance indicators (KPIs). Section 3 covers the technical results (Section 3.1) and the economic analysis (Section 3.2), including a sensitivity analysis of the economic outcomes using response surface models to evaluate the impact of key parameters. Finally, Section 4 provides the conclusions and key takeaways of the study.

2. Methods

This work investigates CO₂ emissions abatement strategies for cement plants from a techno-economic perspective. The plants were simulated by means of the gPROMS Process 2023.2.0 software (Siemens, 2024), by solving steady-state material and energy balances.

The Peng-Robinson cubic equation of state was employed to calculate the thermodynamic properties of both the gas and liquid phases. The solid phases, including natural minerals and clinker phases, are assumed to be ideal solid solutions. The correlations used for the estimations of thermodynamic properties were rigorously reviewed and sourced from various references (Bonnickson, 1954; Bonnickson, 1955; Haas et al., 1981; Hanein et al., 2020; Linstrom and Mallard, 2001; McBride et al., 2002), as detailed in the Supplementary Material. For pure water present throughout the process, the IAPWS-95 thermodynamic model (Wagner and Pruß, 2002) was applied, as it is the standard reference for calculating water and steam thermodynamic properties.

Both custom models and gPROMS built-in models were deployed to simulate the process units of the plants (details are in the Supplementary Material). The following sections describe the plant setup of the reference (i.e., unabated) cement plant, and of the low-carbon configurations (i.e., cement plants decarbonised via electrification and carbon capture).

2.1 Reference cement plant configuration

The reference cement plant (Figure 1) employs a state-of-the-art, highly efficient dry process with a five-stage preheater-calciner kiln system equipped with a grate cooler. The plant is coal-fired and has a production capacity typical of a mid-sized European facility, manufacturing 3024 t/d of clinker, corresponding to about 1 Mt/y when assuming a yearly operation of 8000 h/y. This type of process represents the Best Available Technique (BAT) as indicated in the European BREF document (Schorcht et al., 2013).

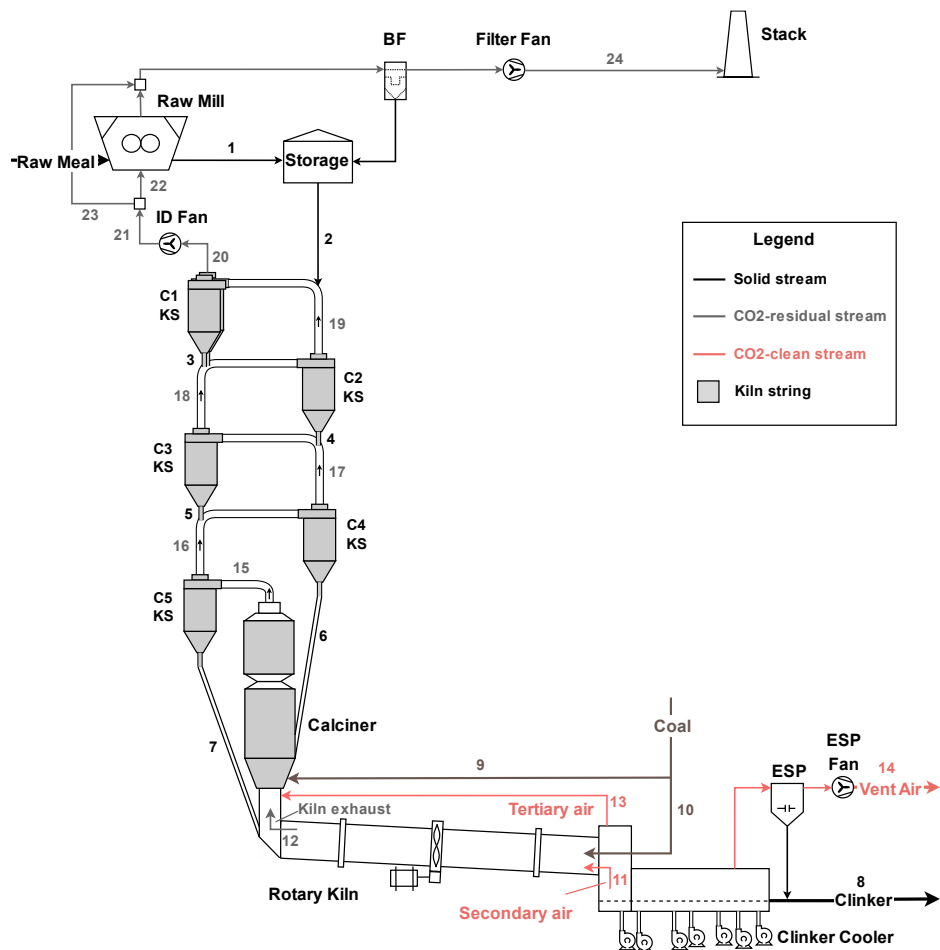


Figure 1. Reference cement plant scheme: modern process with a five-stage preheater-calciner system.

The raw material, referred to as raw meal, consists of CaCO₃, SiO₂, Al₂O₃, Fe₂O₃ and MgCO₃. After being dried and milled in the raw mill, the raw meal enters the five-cyclone preheating tower (stream #2 in Figure 1). Within the tower, exhaust gases from the calciner flow counter-currently with the descending solids through risers and cyclones, cooling to approximately 330°C, while the solids are

heated to around 800°C before being transferred to the calciner (stream #6). The cooled gases (stream #20) are then directed to the raw mill to dry the raw meal.

Within the calciner, the hot tertiary air from the clinker cooler and the kiln exhaust gas are used to burn roughly 60% of the total coal (stream #9) providing the required temperature (870°C) and heat to achieve a calcination rate of 92% (Hewlett and Liska, 2019). The material leaving the lowest cyclone stage (stream #7) descends into the kiln where clinker formation occurs. In this unit, the remaining 40% of the coal (stream #10) is burned with secondary air from the clinker cooler, gradually heating the materials to a peak temperature of 1450°C.

The clinker is cooled to 95°C in the clinker cooler (stream #8), preserving its microstructure and recovering heat for preheating the secondary and tertiary air used in the kiln and calciner.

The key assumptions used for modelling the reference cement plant are provided in the Supplementary Material, along with validation against the plant simulated in Campanari et al. (2016).

2.2 Low-carbon cement plant configurations

The low-carbon configurations are modelled to produce the same output quantity of clinker, namely 3024 t/d. They replace the traditional coal-fuelled calciner with an electrified one, which can be either an Ent- or DT-calciner, as anticipated in Section 1.

The Ent-calciner is a vertical tube where calcination occurs as solids are carried by gas flow along its length from the bottom to the top. It is assumed to be directly electrified through the insertion of heating rods, while the necessary gas flow is provided by recycling a portion of the pure CO₂ produced. Conversely, the DT-calciner is based on the design investigated by LEILAC2 (2023), where calcination occurs within an inner tube, and the heat is transferred indirectly through the calciner wall by an electrical energy source. Here, the solid material moves downward, avoiding the need for CO₂ recycling.

Both electrified calciners are assumed to achieve a calcination rate of 92%, as in the reference plant, by heating the raw meal to 920°C. This is to account for the increased CO₂ partial pressure, following

similar studies on oxyfuel or electrified calciners (De Lena et al., 2019; Quevedo Parra and Romano, 2023). The electrical power required for the calciner is calculated assuming a 95% electricity-to-heat efficiency (Wilhelmsen et al., 2018). The remaining calcination and clinker formation reactions occur in a coal-fired kiln, which maintains the same design and secondary air flowrate as the reference plant.

This setup enables the capture of CO₂ released during calcination, which can then be directed to a CO₂ compression and purification unit (CPU) before transportation and storage. To maintain the purity of the CO₂-rich stream from the electrified calciner, modifications to the typical system are necessary. Since fuel combustion is no longer needed, the supply of coal and tertiary air to the calciner (stream #9 and stream #13 in Figure 1) is removed. The supply of exhaust gas from the kiln (stream #12) is also eliminated because it would merely dilute the CO₂ stream. The absence of coal combustion alters the fuel ash contribution to clinker composition in the low-carbon scenarios. To maintain consistent clinker chemistry with the reference case, the raw meal chemistry is adjusted accordingly, as presented in Table 1.

Table 1. Raw meal composition after drying for the reference plant and the low-carbon designs.

Species	Reference plant (% mass wet)	Low-carbon designs (% mass wet)
CaCO ₃	78.91	78.45
SiO ₂	13.74	13.98
Al ₂ O ₃	3.32	3.52
Fe ₂ O ₃	2.00	2.01
MgCO ₃	1.53	1.54
H ₂ O (Moisture)	0.50	0.50

Another major modification regards the heat recovery strategy for the hot CO₂ produced, leading to a significant distinction in configuration. Following Quevedo Parra and Romano (2023) and Jacob and Tokheim (2023), two design options can be envisaged: the heat content of the CO₂-rich stream can either be used to preheat the raw meal (RMP configuration) or be transferred to a fraction of the vent air from the clinker cooler via a gas-gas heat exchanger (GGHX configuration). The two alternatives are detailed in the following:

- **RMP configuration:** The CO₂-rich stream preheats a portion of the raw meal in a new calciner string, with three cyclone stages. Kiln exhaust gas, mixed with a fraction of tertiary air from the cooler, preheats the remaining raw meal in the kiln string, also consisting of three cyclones. The flowrate of tertiary air diverted to the kiln string is tuned so that the raw meal is heated to 765°C before entering the calciner, preventing premature calcination. Air leakage (i.e., false air) into the cyclones might reduce the CO₂ concentration below transportation specifications. It is assumed that false air ingress in cyclones could be reduced by 80% through improved construction and maintenance.
- **GGHX configuration:** The heat content of the CO₂-rich stream is transferred to a fraction of the vent air from the clinker cooler via a gas-gas heat exchanger. Subsequently, the heated vent air is mixed with kiln exhaust gas and tertiary air, preheating the raw meal in a four-stage cyclone tower. The re-routed portion of vent air is calculated to match the gas mass flow entering the preheating tower of the reference plant, while its outlet temperature is regulated to maintain a maximum temperature of 765°C at the bottom of the kiln string.

The two methods of handling the CO₂ stream, combined with the two calciner types, result in the four processes investigated in this study (Table 2), which are further discussed in the following. For further information on the modelling assumptions, the reader is referred to the Supplementary Material.

Table 2. Summary of the key differences between the low-carbon designs.

Configuration	Calciner technology	Heat recovery strategy CO ₂
DT-RMP	Drop tube (without CO ₂ recycle)	Raw meal preheating in calciner string
Ent-RMP	Entrainment (with CO ₂ recycle)	Raw meal preheating in calciner string
DT-GGHX	Drop tube (without CO ₂ recycle)	Vent air heating via gas-gas heat exchanger
Ent-GGHX	Entrainment (with CO ₂ recycle)	Vent air heating via gas-gas heat exchanger

Note that the calciner electrification addresses only the CO₂ emissions related to the calcination reaction and coal combustion within the calciner. However, the rotary kiln remains coal-fired, and a certain amount of CO₂ would still be emitted. Consequently, an additional post-combustion carbon capture (PCC) technology is integrated into the processes to mitigate these emissions. Among the various options, MEA-based carbon capture was chosen due to its maturity (Schneider et al., 2023)

and the availability of significant waste heat for MEA regeneration in low-carbon processes. Furthermore, it is assumed that every process includes a suitable selective non-catalytic reduction (SNCR) unit to abate NO_x from coal combustion.

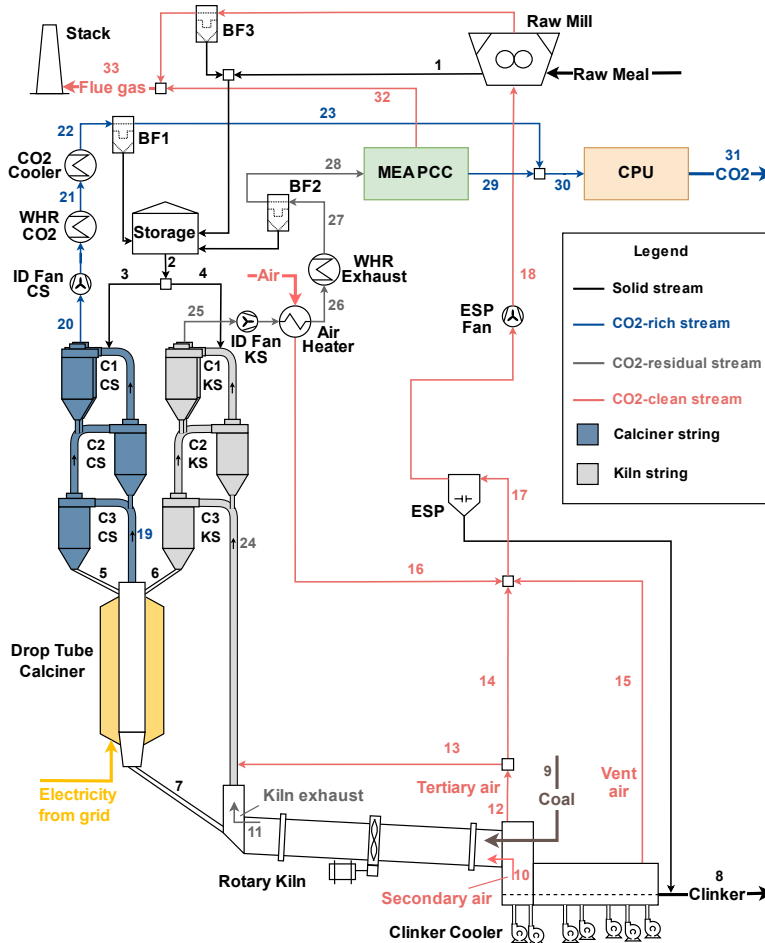


Figure 2. DT-RMP configuration scheme: drop tube calciner with pure CO₂ preheating raw meal.

DT-RMP (Figure 2): this configuration involves a DT-calciner where the pure CO₂ is utilised to preheat the raw meal in the calciner string. The raw meal split to this tower is specified to have the CO₂ stream at a temperature of 400°C (stream #20 in Figure 2). This stream undergoes a waste heat recovery step before cooling down to 60°C by means of cooling water. The cold CO₂ is then cleaned of any entrained dust in a bag filter (BF) and sent to the CPU.

The exhaust gas exiting the kiln string (stream #25) still contains a moderate CO₂ concentration (approximately 10% mol). To make the MEA capture process less energy- and capital-intensive, this stream is not used for raw meal drying because it would be diluted. Therefore, to cover the heat duty for drying, a mix of the residual tertiary air (stream #14), vent air (stream #15), and additional hot air

(stream #16) is used. The latter is heated to 250°C by the kiln string flue gas (stream #25), from which waste heat is recovered before it is sent to MEA PCC.

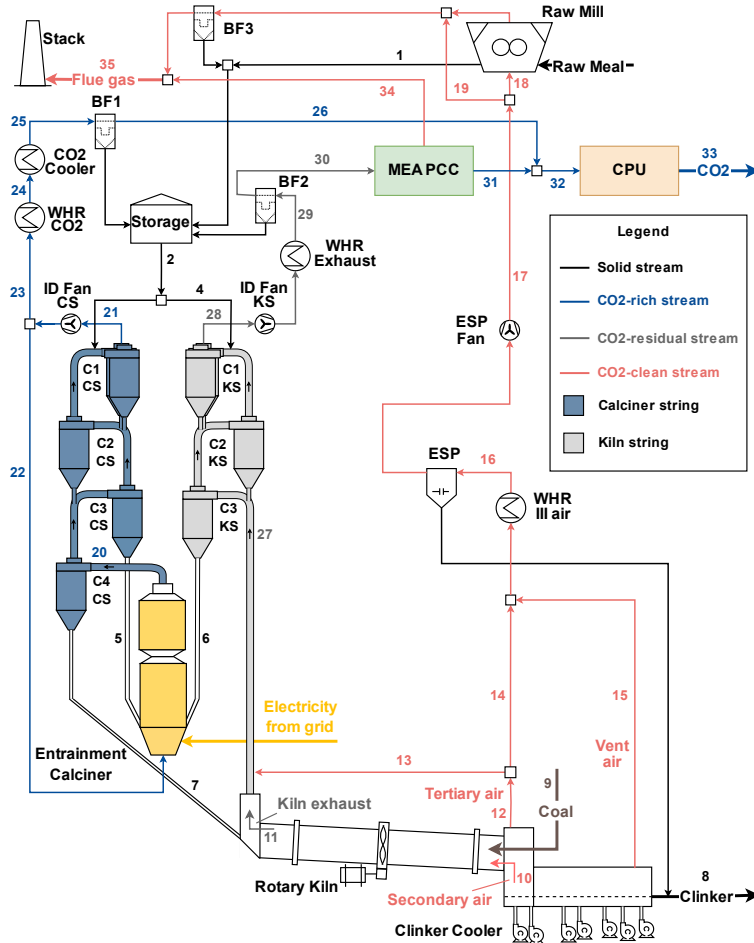


Figure 3. Ent-RMP configuration scheme: entrainment calciner with pure CO₂ preheating raw meal.

Ent-RMP (Figure 3): this alternative considers an Ent-calciner with raw meal preheating by the CO₂-rich stream in the calciner string. A portion of the CO₂-rich stream is recycled back to the calciner (stream #22 in Figure 3) to provide the necessary gas flow to lift the solid particles. The recycling is assumed to maintain 50% of the volumetric flow rate at the calciner entrance in the reference plant. This results in a larger gas flowrate circulating in the calciner string and a loss in thermal efficiency with respect to a DT-calciner. Hence, the temperature at the top of the calciner string (stream #21) is set to 530°C to reduce the energy loss, but still retains a reasonable operating temperature for the fan.

The pure CO₂ (stream #23) undergoes waste heat recovery and further cooling, followed by dust removal via a bag filter, before being sent to the CPU. In this design configuration, the total heat

content of the residual tertiary and vent air is sufficient for coal and raw meal drying. This mixture is cooled to 400°C to avoid operational issues within the electrostatic precipitator (ESP) and used for drying purposes. The flue gas from the kiln string (stream #28) undergoes heat recovery and dust cleaning before the final MEA capture and CPU steps.

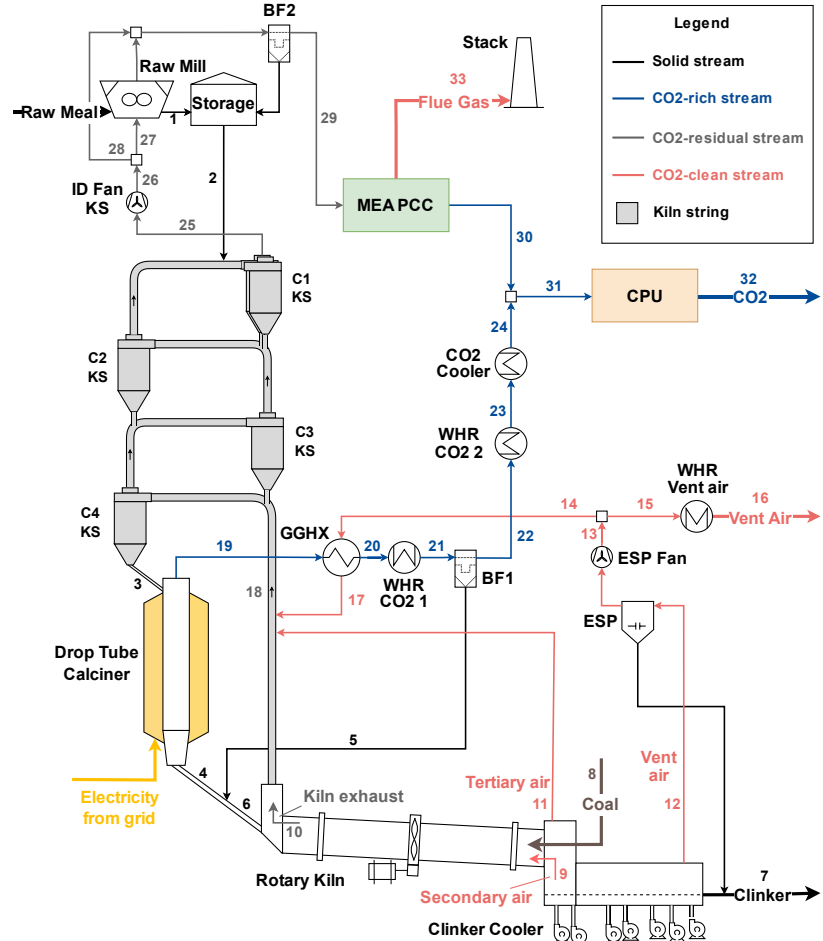


Figure 4. DT-GGHX configuration scheme: drop tube calciner with pure CO₂ preheating vent air via a gas-gas heat exchanger.

DT-GGHX (Figure 4): this configuration employs a DT-calciner where the heat from the hot CO₂ (stream #19 in Figure 4) is extracted in a gas-gas heat exchanger to preheat a fraction of the vent air from the clinker cooler (stream #14). After exiting the gas-gas heat exchanger, the CO₂ is cooled down to 250°C (which allows using a bag filter) by producing low-pressure steam. In the bag filter, the entrained calcined material is recovered and returned to the rotary kiln, while the CO₂ moves to additional waste heat recovery and cooling steps, before entering the CPU.

The CO₂ concentration of the flue gas is approximately 5% mol after the kiln string (stream #25). These hot gases are further deployed for raw meal drying, which is an efficient solution as the heat from the residual vent air (stream #15) is adequate for coal drying but insufficient for raw meal drying. After drying, the gas (stream #29) is sent to the downstream MEA absorption unit to capture the residual CO₂ and then to the CPU.

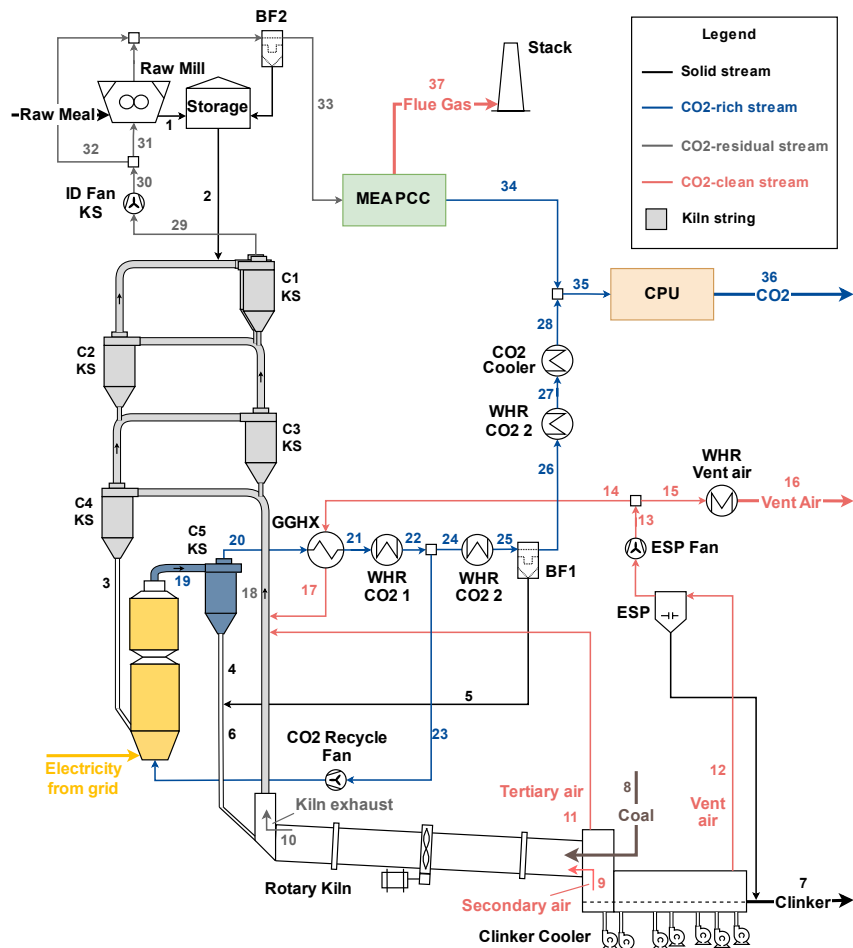


Figure 5. Ent-GGHX configuration scheme: entrainment calciner with pure CO_2 preheating vent air via a gas-gas heat exchanger.

Ent-GGHX (Figure 5): this option involves an Ent-calciner with heat integration between the pure CO₂ stream and a share of the vent air, similar to the DT-GGHX design. As in the Ent-RMP case, pure CO₂ (stream #20 in Figure 5) is cooled down to 530°C through waste heat recovery and split into two streams. A portion is recycled back to the Ent-calciner to provide the necessary gas flow (stream #23), while the remaining fraction (stream #24) is further cooled to the operating temperature

of the bag filter, where the calcined material is recovered. Subsequently, it is cooled down to 60°C before entering the CPU.

For raw meal drying purposes, the same approach as in the DT-GGHX alternative is applied. Therefore, the hot gas from the kiln string (stream #29) is utilised to dry the raw meal. The gas stream is then de-dusted, sent to the MEA PCC, and finally to the CPU.

2.3.1 MEA PCC modelling

The MEA PCC process is modelled as a black box unit, based on the findings of Sanchez Fernandez et al. (2014). It assumes a 90% capture rate, with energy requirements varying by case, as shown in Table 3. This study was selected because it evaluated the MEA PCC process at two different CO₂ molar concentrations (13.7% and 4.0%), which align with the CO₂ molar concentrations of the stream fed to the MEA capture in the low-carbon scenarios (9.2%, 12.9%, 3.9% and 3.8%).

Table 3. MEA-based carbon capture assumptions for the low-carbon configurations.

Case	Capture rate (%)	% mol CO ₂ feed MEA PCC	Spec. reboiler duty (MJ _{th} /kgCO ₂)	Spec. power auxiliaries (MJ _{el} /kgCO ₂)
DT-RMP	90	9.2	3.70	0.15
Ent-RMP	90	12.9	3.70	0.15
DT-GGHX	90	3.9	3.95	0.27
Ent-GGHX	90	3.8	3.95	0.27

The heat required for amine regeneration is supplied by low-pressure steam (3.15 bar) at 135°C, generated through a waste heat recovery. The system is designed to avoid heat recovery below 160°C, ensuring a minimum temperature approach of 25°C in the evaporators. If steam production is insufficient (as the results will show, cases DT-RMP and DT-GGHX), supplementary heat is provided by an air-sourced heat pump with a coefficient of performance (COP) of 2 (Arpagaus et al., 2018; d'Amore et al., 2023), ensuring consistency with the electrification approach.

This study adopts the “Moderate Purity” CO₂ quality specifications outlined by Magli et al. (2022). The CPU design is based on those suggested by Anantharaman et al. (2017) and Magli et al. (2022), with further details provided in the Supplementary Material.

2.3 KPIs and economic analysis

The environmental and economic performance of the investigated processes are evaluated using a series of KPIs, as outlined in Equations 1-7.

The equivalent specific CO₂ emissions ($e_{eq,clk}$ [kgCO₂/t_{clk}]) are calculated as:

$$e_{eq,clk} = e_{clk} + e_{el,clk} \cdot (1)$$

where e_{clk} represent direct CO₂ emissions (Scope 1) and $e_{el,clk}$ reflects indirect CO₂ emissions associated to the electricity supplied to the plant (Scope 2). The latter is computed as the sum of the electrical energy consumption of the process ($P_{el,clk}$ [MWh_{el}/t_{clk}]) and the carbon intensity of the imported electricity (e_{el} [kgCO_{2,eq}/MWh_{el}]):

$$e_{el,clk} = P_{el,clk} \cdot e_{el} \quad (2)$$

The carbon capture rate (CCR [%]) indicates the CO₂ capture efficiency by measuring the amount of carbon effectively captured (and sent to storage) relative to the total amount generated by the process, excluding indirect emissions. It is defined as:

$$CCR = \frac{e_{capt,clk}}{e_{capt,clk} + e_{clk}} \cdot 100 \cdot (3)$$

where $e_{capt,clk}$ [kgCO₂/t_{clk}] is the amount of CO₂ captured. To include indirect emissions in the analysis, the equivalent CO₂ avoided (AC_{eq} [%]) metric evaluates CO₂ reduction by comparing equivalent emissions between the low-carbon plant and the reference plant:

$$AC_{eq} = \left(1 - \frac{e_{eq,clk}^{decarb}}{e_{eq,clk}^{ref}} \right) \cdot 100 \cdot (4)$$

where the superscript "decarb" refers to the plant with decarbonisation measure, and "ref" to the unabated reference plant.

Two scenarios are evaluated for the carbon intensity of imported electricity. The first scenario reflects the EU-27 energy mix, based on the latest available data from 2022, with $e_{el} = 258$ kgCO_{2,eq}/MWh_{el} (EEA, 2024). The second scenario assumes electricity supplied entirely from non-combustible

renewables (wind, solar and hydro), thus setting $e_{el} = 0$ kgCO_{2,eq}/MWh_{el}. Notably, these carbon intensity values exclude upstream emissions associated with the electricity supply chain.

The economic analysis methodology presented in this study follows best practices for cost estimation in CCS projects, as outlined by Rubin et al. (2013) and van der Spek et al. (2019). The assessment requires estimating the capital costs (CAPEX) and operating costs (*OPEX* [€/y]) for the investigated processes, resulting in two economic KPIs: the cost of clinker (*CO_C* [€/t_{clk}]) and the cost of avoided CO₂ (*CAC* [€/t_{CO₂}]). They are defined as follows:

$$CO_C = \frac{TAC + OPEX}{\dot{m}_{clk}} \quad (5)$$

$$CAC = \frac{CO_C^{decarb} - CO_C^{ref}}{e_{eq,clk}^{ref} - e_{eq,clk}^{decarb}}, \quad (6)$$

where *TAC* [€/y] is the total annualised CAPEX and \dot{m}_{clk} [t_{clk}/y] is the annual clinker productivity.

All costs are expressed in €₂₀₂₄, adjusted using the CEPCI for January 2024, which is 795.4 (Chemical Engineering, 2024), and assuming a US Dollar to Euro conversion rate of 0.91. The baseline *CAC* calculations assume a grid carbon intensity of 258 kgCO_{2,eq}/MWh_{el} for the EU-27 in 2022.

A bottom-up approach, typical of preliminary cost analysis is employed for the evaluation of CAPEX (Rubin et al., 2013). This involves computing the total overnight cost (*TOC* [€]) of the plant, starting from the equipment cost of individual units (*EC* [€]), as illustrated in Figure 6 and explained in the following.

The estimation of *EC* for a generic unit *j* is based on its key features derived from process simulations and design criteria, using various cost correlations (Cinti et al., 2018; d'Amore et al., 2023; De Lena et al., 2019; Gardarsdottir et al., 2019; IEAGHG, 2013; Magli et al., 2022; Manzolini et al., 2015; Mastropasqua et al., 2019; NETL, 2019; Turton et al., 2018).

A suitable installation factor (*IF* [–]) is applied to *EC* to determine the bare erected cost (*BEC* [€]) of the equipment, accounting for the installation cost. Depending on the maturity of the technology and the level of detail in the equipment list, a process contingency is applied as a percentage of the

BEC, yielding the total direct cost (*TDC* [€]) of the unit. A detailed survey of all cost correlations, installation factors and process contingencies used in this study is provided in the Supplementary Material.

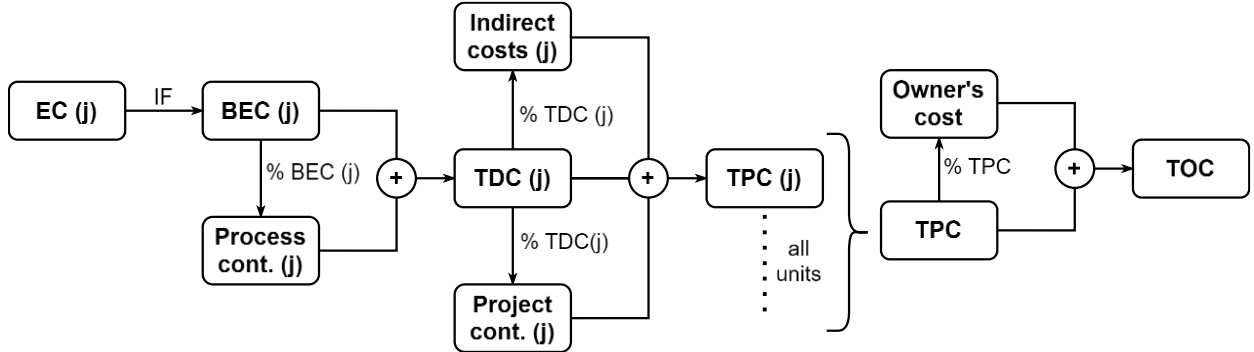


Figure 6. Diagram of calculation procedure to estimate plant CAPEX.

To obtain the total plant cost (*TPC* [€]) of each item, indirect costs and project contingencies are added as a percentage of *TDC*. Based on Gardarsdottir et al. (2019), indirect costs are set at 14% of *TDC*, and project contingencies are 15% of *TDC* for the reference plant. For low-carbon cases, project contingencies are increased to 20% of *TDC* to account for the higher risks associated with emerging CCS technologies. The summation of *TPC* of each unit represents the plant CAPEX including direct and indirect costs, to which the owner's costs (e.g., land, inventory and start-up capital) must be added. Owner's costs of 10% of the *TPC* are applied to obtain the *TOC*. Finally, the *TOC* are annualised to *TAC* with Equation 10, assuming a plant operational life (*n*) of 25 years and a discount rate (*i*) equal to 8%:

$$TAC = TOC \cdot \frac{i(1+i)^n}{(1+i)^n - 1} \quad (7)$$

The *OPEX* are divided into fixed and variable costs, with the assumptions for their calculations summarised in Table 4. The operating labour cost (*OL* [€/y]) is calculated by multiplying the labour cost by the number of employees at the plant. *OL* and maintenance labour (*ML* [€/y]), which constitutes 40% of the total maintenance cost, contribute to the estimation of administrative/support labour costs.

Table 4. Assumptions for OPEX calculation

Fixed OPEX		Reference
Local taxes/insurance	% TPC/y	2.0
Maintenance	% TPC/y	2.5
Personnel in reference plant	-	100
Additional personnel in capture plant	-	20
Labour Cost	€/year per personnel	60000
Maintenance labour (ML)	% Maintenance	40
Administrative/support labour	% (OL + ML)	30

Variable OPEX		Reference
Raw Meal	€/t _{Raw Meal}	3.012
Coal	€/GJ _{LHV}	3.00
Electricity	€/MWh _{el}	125.0
Steam (from waste heat)	€/MWh _{th}	8.5
Cooling water (30-40°C)	€/m ³	0.02
Refrigerated water (15-25°C)	€/m ³	0.14
Process water	€/m ³	6.65
Ammonia SNCR	€/t _{NH3}	130.0
MEA	€/t _{MEA}	1450.0
NaOH DeSOx	€/t _{NaOH}	370.0
CO ₂ Transport and Storage	€/t _{CO₂,capt}	35.0

It is important to note that no carbon tax (c_{CO_2} [€/t_{CO₂}]) on the emitted CO₂ is applied in the baseline analysis. However, this study assesses sensitivity to this parameter. When a carbon tax is applied, the electricity cost (c_{el} [€/MWh_{el}]) is updated as:

$$c_{el} = c_{el,base} + \frac{c_{CO_2} \cdot e_{el}}{1000} \quad (11)$$

where the base cost of electricity ($c_{el,base}$) is the EU-27 average value for non-household consumers (IG band) in the second semester of 2023 (Eurostat, 2024).

3. Results and discussion

3.1 Techno-environmental results

The heat and electrical energy demands for the reference plant and the low-carbon scenarios are compared in Table 5. The heat duty for the calciner increases in all the low-carbon cases compared to the reference (between +12% and +32%), as the temperature needed to achieve a 92% calcination

rate is raised from 870°C to 920°C in a pure CO₂ atmosphere. Consequently, the heat requirements of the rotary kiln decrease (between -15% and -11%) because the calcined meal enters the kiln at a higher temperature with the same calcination rate.

Table 5. Summary of fuel consumptions, heat and electricity demands for reference cement plant and low-carbon configurations. DT-RMP = drop tube calciner with pure CO₂ preheating raw meal; Ent-RMP = entrainment calciner with pure CO₂ preheating raw meal; DT-GGHX = drop tube calciner with pure CO₂ preheating vent air via a gas-gas heat exchanger; Ent-GGHX = entrainment calciner with pure CO₂ preheating vent air via a gas-gas heat exchanger.

	Reference plant	DT-RMP	Ent-RMP	DT-GGHX	Ent-GGHX
Heat duty cement process					
Heat duty calciner	GJ _{LHV/t_{clk}}	1.89	2.15	2.44	2.11
Heat duty kiln	GJ _{LHV/t_{clk}}	1.23	1.06	1.04	1.09
Direct fuel consumption	GJ_{LHV/t_{clk}}	3.13	1.06	1.04	1.09
Change w/r to reference plant	-	-66.2%	-66.6%	-65.2%	-65.0%
Heat duty MEA capture					
Heat duty MEA regeneration	GJ _{LHV/t_{clk}}	-	0.50	0.48	0.56
Waste heat available ^a	GJ _{LHV/t_{clk}}	-	0.21	0.51	0.25
Net heat duty MEA regeneration	GJ _{LHV/t_{clk}}	-	0.29	- ^b	0.31
Total heat duty	GJ_{LHV/t_{clk}}	3.13	3.51	3.48	3.51
Change w/r to reference plant	-	12.1%	11.4%	12.1%	15.0%
Overall electrical energy demand					
Electrified calciner ^c	GJ _{el/t_{clk}}	-	2.27	2.57	2.22
MEA heat pump ^d	GJ _{el/t_{clk}}	-	0.15	0.00	0.15
MEA auxiliaries	GJ _{el/t_{clk}}	-	0.02	0.02	0.04
CPU	GJ _{el/t_{clk}}	-	0.23	0.24	0.23
Cement plant auxiliaries	GJ _{el/t_{clk}}	0.47	0.48	0.49	0.49
Total electricity	GJ_{el/t_{clk}}	0.47	3.15	3.31	3.14
	MW_{el}	16.58	110.30	115.91	109.95
Change w/r to reference plant	-	565.1%	599.0%	563.0%	620.0%

^a Assumed to be recovered from hot streams down to 160°C

^b Waste heat available is sufficient to cover the MEA regeneration heat duty entirely. The excess waste heat is minimal and will not significantly impact the technical analysis.

^c Computed assuming electricity-to-heat efficiency of 95%

^d Computed assuming a COP equal to 2

The DT-calciner configurations exhibit a lower calciner heat demand than Ent-calciner ones (2.11 and 2.15 against 2.44 and 2.50 GJ_{LHV/t_{clk}}) due to the energy penalty of re-heating the CO₂ flow recycled to lift the solids. However, a larger amount of waste heat can be recovered when the Ent-calciner is installed, which is sufficient to cover the entire thermal requirements of the MEA capture.

This is not the case for DT-RMP and DT-GGHX cases, where the available waste heat meets 42% and 45% of thermal demand for MEA regeneration, respectively, necessitating a heat pump to provide the remaining duty to operate the MEA PCC.

As expected, the low-carbon processes demonstrate a substantial increase in electrical energy demand, with the electricity consumption significantly higher than the reference cement plant by factors of 5.6, 5.7, 6, and 6.2 for DT-GGHX, DT-RMP, Ent-RMP, and Ent-GGHX, respectively. This increase is due to the electrification of the calciner (71-78% of total electrical demand), MEA capture (1-6% of total electrical demand), and CPU sections (7% of total electrical demand).

Among the low-carbon processes, the major difference in electrical requirements is related to the different calciner duties. The estimated electrical power at the calciner is 79.3 MW_{el} for DT-RMP, 89.9 MW_{el} for Ent-RMP, 77.8 MW_{el} for DT-GGHX, and 92.2 MW_{el} for Ent-GGHX. Additionally, DT-RMP and DT-GGHX configurations require additional electrical power for the heat pump (5.1-5.4 MW_{el}), while the CPU shows similar energy requirements for all cases (8.2-8.4 MW_{el}).

Detailed stream tables for the reference plant and the low-carbon processes are provided in the Supplementary Material.

The environmental KPIs, computed under the two carbon intensity scenarios for electricity as described in Section 2, are summarised in Table 6. All configurations exhibit very high *CCR* of approximately 97.5%. When considering the same heat recovery strategy for the CO₂-rich stream, alternatives employing DT-calciner show better energy efficiency compared to those with Ent-calciner. Specifically, DT-calciners achieve a comparable *CCR* with similar fuel consumption while requiring less electricity.

Under an EU-27 energy mix scenario, *AC_{eq}* ranges between 70 and 72%, with only minor differences observed among the low-carbon configurations. DT-calciner designs demonstrate slightly better performance than Ent-calciner ones, primarily due to their lower electrical power demand, which translates into reduced indirect emissions. Overall, under these assumptions, the *AC_{eq}* results for all the configurations are not competitive with those of an oxyfuel cement plant (*AC_{eq}* = 81.5%) or an

integrated calcium looping technology ($AC_{eq} = 88.3\%$) (Voldsgaard et al., 2019). This is notable considering that the investigated low-carbon scenarios achieve a significantly higher *CCR* (about 97.5% in this study, compared to 90% for oxyfuel and calcium looping in Voldsgaard et al., 2019).

Table 6. Summary of environmental key performance indicators for reference cement plant and low-carbon configurations under different scenarios for the carbon intensity of electricity. DT-RMP = drop tube calciner with pure CO_2 preheating raw meal; Ent-RMP = entrainment calciner with pure CO_2 preheating raw meal; DT-GGHX = drop tube calciner with pure CO_2 preheating vent air via a gas-gas heat exchanger; Ent-GGHX = entrainment calciner with pure CO_2 preheating vent air via a gas-gas heat exchanger.

	Reference plant	DT-RMP	Ent-RMP	DT-GGHX	Ent-GGHX
Direct fuel consumption	GJ _{LHV} /t _{clk}	3.13	1.06	1.04	1.09
Electric power consumption ($P_{el,clk}$)	MWh _{el} /t _{clk}	0.132	0.875	0.920	0.873
CO_2 captured ($e_{capt,clk}$)	kg CO_2 /t _{clk}	0.0	630.6	630.0	633.4
Direct CO_2 emissions (e_{clk})	kg CO_2 /t _{clk}	833.1	16.4	15.5	15.8
CO_2 outlet purity	% mol (dry)	-	99.0%	97.7%	99.4%
Carbon capture rate (CCR)	%	-	97.5%	97.6%	97.6%
EU-27 energy mix in 2022 ($e_{el} = 258$ kg $CO_{2,eq}$ /MWh _{el})					
Indirect CO_2 emissions ($e_{clk,el}$)	kg CO_2 /t _{clk}	34.0	225.9	237.3	225.1
Equivalent CO_2 emissions ($e_{clk,eq}$)	kg CO_2 /t _{clk}	867.1	242.3	252.8	241.0
Equivalent CO_2 avoided (AC_{eq})	%	-	72.0%	70.8%	72.2%
Non-combustible renewables ($e_{el} = 0$ kg $CO_{2,eq}$ /MWh _{el})					
Indirect CO_2 emissions ($e_{clk,el}$)	kg CO_2 /t _{clk}	0.0	0.0	0.0	0.0
Equivalent CO_2 emissions ($e_{clk,eq}$)	kg CO_2 /t _{clk}	833.1	16.4	15.5	15.8
Equivalent CO_2 avoided (AC_{eq})	%	-	98.0%	98.1%	98.1%

Due to the absence of indirect emissions, the AC_{eq} index improves substantially in a scenario where the plant electrical demand is supplied by renewable energy, with values above 98% and identical for all the configurations. In this context, the proposed processes are competitive with oxyfuel plants and plants with integrated calcium looping technology, which have AC_{eq} of 89.4% and of 93.2%, respectively (Voldsgaard et al., 2019).

The contribution of direct, indirect and captured CO_2 emissions to the equivalent emissions under the two electricity carbon intensity scenarios is illustrated in Figure 7.

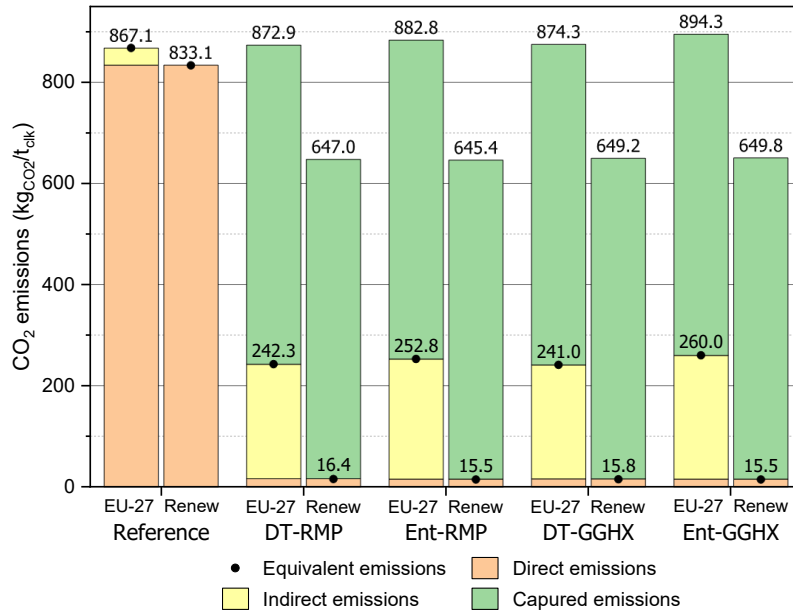


Figure 7. Breakdown of CO₂ emissions for reference cement plant and low-carbon configurations under different scenarios for the carbon intensity of electricity. EU-27: carbon intensity electricity = 258 kgCO₂/MW_{el}; Renew: carbon intensity electricity = 0 kgCO₂/MW_{el}.

DT-RMP = drop tube calciner with pure CO₂ preheating raw meal; Ent-RMP = entrainment calciner with pure CO₂ preheating raw meal; DT-GGHX = drop tube calciner with pure CO₂ preheating vent air via a gas-gas heat exchanger; Ent-GGHX = entrainment calciner with pure CO₂ preheating vent air via a gas-gas heat exchanger.

The captured and direct emissions from low-carbon processes remain constant across both scenarios. Notably, under the EU-27 energy mix, the total emissions of low-carbon plants are slightly higher than those of the unabated plant, despite a 66% reduction in fuel combustion. This is due to the high indirect emissions associated with carbon-intensive electricity, resulting in still significant equivalent emissions (242-260 kgCO₂/t_{ck}). This underscores that these processes only reduce emissions when low-carbon electricity is utilised. In fact, when renewable energy sources are employed, the total emissions in low-carbon configurations decrease by an average of 22% compared to the unabated plant, with equivalent emissions dropping as low as 16 kgCO₂/t_{ck}.

3.2 Economic results

The total plant cost (*TPC*) breakdown across different equipment categories is illustrated in Figure 8. The low-carbon configurations exhibit a marked increase in *TPC* compared to the reference plant, with costs rising from 98 M€ for Ent-RMP (+36%) up to 224 M€ for DT-GGHX (+83%). This cost increase is primarily driven by the addition of units such as the MEA capture system, the CPU, and

the electrified calciner, which are the major contributors. At the same time, the new low-carbon designs involve some costs reduction associated with the coal mill and SNCR due to the reduced coal consumption. However, these savings are not sufficient to offset the increase in *TPC* of low-carbon alternatives compared to the reference unabated cement plant.

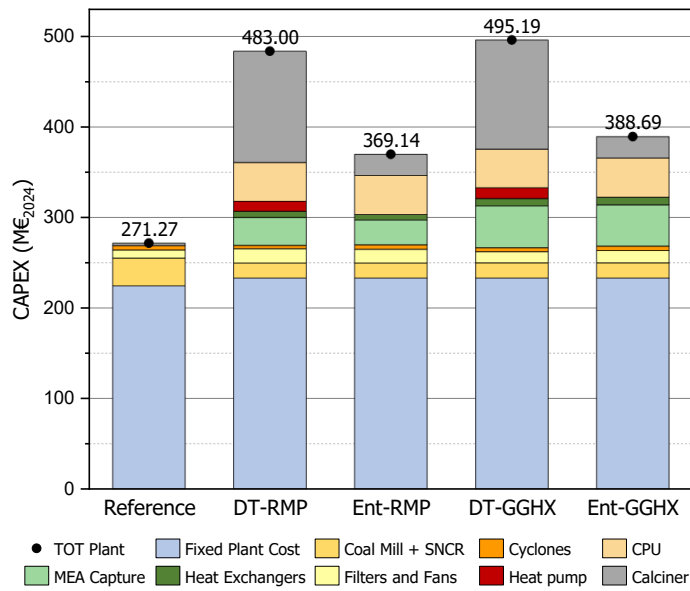


Figure 8. Breakdown of total plant cost for reference cement plant and low-carbon configurations. DT-RMP = drop tube calciner with pure CO₂ preheating raw meal; Ent-RMP = entrainment calciner with pure CO₂ preheating raw meal; DT-GGHX = drop tube calciner with pure CO₂ preheating vent air via a gas-gas heat exchanger; Ent-GGHX = entrainment calciner with pure CO₂ preheating vent air via a gas-gas heat exchanger.

DT-calciner configurations are the most capital-intensive, mainly due to two key factors: (i) the DT-calciner itself is significantly more expensive, with an estimated *TPC* of 120 M€, compared to 24 M€ for the Ent-calciner; (ii) the DT-calciner designs require the installation of an 11 M€ electric heating system based on heat pumps, which is not needed in the Ent-calciner processes, as the latter can recover sufficient heat internally to the process.

Comparing processes with the same type of calciner, RMP configurations exhibit lower capital expenditures than GGHX ones due to the more cost-effective MEA capture process. In fact, the CO₂ stream sent to MEA capture, while similar in flowrate, is more concentrated, leading to smaller and less expensive equipment. Other process sections do not exhibit significant cost differences among the alternatives.

The breakdown of the cost of clinker (*COC*) for the reference cement plant and the low-carbon configurations is reported in Figure 9a. Variable OPEX is a major contributor, accounting for 63-70% of the total *COC*, depending on the configuration. The total annualised CAPEX (*TAC*) represents approximately 18% of the *COC* in Ent-calciner processes and around 22% in DT-calciner processes. The remaining share is attributed to fixed OPEX, which follows the same trend as CAPEX since it is calculated based on *TPC*.

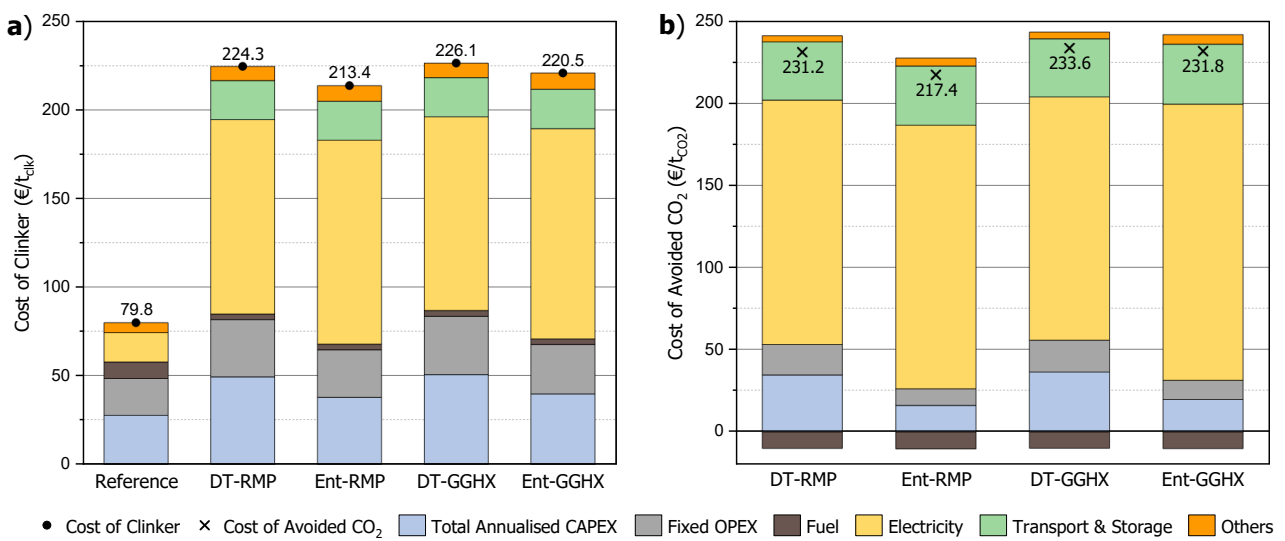


Figure 97. Breakdown of (a) cost of clinker and (b) cost of avoided CO₂ for reference cement plant and low-carbon configurations. DT-RMP = drop tube calciner with pure CO₂ preheating raw meal; Ent-RMP = entrainment calciner with pure CO₂ preheating raw meal; DT-GGHX = drop tube calciner with pure CO₂ preheating vent air via a gas-gas heat exchanger; Ent-GGHX = entrainment calciner with pure CO₂ preheating vent air via a gas-gas heat exchanger.

Figure 9a clearly shows that electricity costs dominate the total *COC*, due to both the high baseline electricity prices assumed and the significant electrical energy demand of the processes. Electricity costs account for 49%, 54%, 48%, and 54% of the total *COC* for DT-RMP, Ent-RMP, DT-GGHX, and Ent-GGHX, respectively. Additionally, CO₂ transportation and storage costs have a significant impact on the *COC*, accounting for about 10% of the total. Other costs are related to raw meal purchase and the various utilities required for plant operations, such as cooling, refrigerated and process water, steam management, and make-ups for NH₃, MEA, and NaOH, and account for up to 4% of the total.

Ent-RMP has the best economic performance, although the *COC* is still 2.67 times higher than that of the reference plant, followed by the Ent-GGHX, DT-RMP, and DT-GGHX configurations, with *COC* increases of 2.76, 2.81, and 2.83 times, respectively.

The cost of avoided CO₂ (*CAC*) breakdown in Figure 9b resembles that of *COC*, leading to similar observations. In this case, the dominance of electricity costs is even more pronounced, representing 64%, 74%, 63%, and 72% of the total *CAC* for DT-RMP, Ent-RMP, DT-GGHX, and Ent-GGHX, respectively.

Ent-RMP also stands out in terms of *CAC*, making it the most economically favourable configuration, while Ent-GGHX does not perform as well, with a *CAC* comparable to that of the DT-calciner designs, because of its higher equivalent CO₂ emission.

The *CAC* reflects the carbon tax required to break even with the production costs of the reference plant without mitigation measures. This relationship is highlighted in the sensitivity analysis of the *COC* to carbon tax for the reference plant and low-carbon designs, as presented in Figure S16 of the Supplementary Material.

Compared to the EU Emission Trading System price of approximately 70 €/tCO₂ in August 2024 (Ember, 2024), the *CAC* for all configurations is notably high. This is largely due to the high electricity price in Europe, which was selected as the nominal value (125 €/MWh_{el}), with the significant rise in electricity demand making energy cost the most critical factor influencing the economic feasibility of these technologies. Additionally, grid carbon intensity significantly impacts the *CAC*, particularly in electrified processes where indirect emissions become more relevant. It is important to emphasise that the cost estimates for the electrified calciner are highly uncertain, as no industrial demonstrations currently exist. Further analyses were conducted to investigate how variations in these key parameters affect the economic performance of low-carbon scenarios.

3.2.1 Sensitivity analyses on economic performance

A sensitivity analysis was conducted to assess the combined effects of electricity price, carbon intensity of imported electricity, and electrified calciner cost on *CAC*. Simulated data were generated to explore the parameter space outlined in Table 7, using a three-level full factorial Design of Experiments. A response surface model was then developed to investigate the effects of individual factors, their interactions, and quadratic effects by estimating the associated regression coefficients.

Table 7. Factor levels of the Design of Experiments used for the sensitivity analysis.

Parameter		Low level	Intermediate level	High level
Electricity price	€/MWh _{el}	0	100	200
CO ₂ intensity electricity	kgCO _{2,eq} /MWh _{el}	0	200	400
Δ calciner cost	%	-50	0	50

The upper limit for electricity price is set at 200 €/MWh_{el}, reflecting the peak prices observed in Europe during 2022 (Eurostat, 2024). The upper bound for grid CO₂ intensity is 400 kgCO_{2,eq}/MWh_{el}, representing the average emission factor for a natural gas power plant (IEA, 2019).

The analysis results are presented in contour plots (Figure 10), illustrating the variation in *CAC* as a function of electricity price (*x*-axis) and grid CO₂ intensity (*y*-axis) across three levels of calciner cost variation (-50%, 0%, and +50%) for the four low-carbon configurations.

The plots reveal the direct proportionality between *CAC* and the analysed factors, as well as the interaction between electricity price and carbon intensity. The effect of electricity price is particularly significant when both carbon intensity and electricity price are at their lower levels (bottom-left corner), as indicated by the nearly vertical contour lines. As these parameters increase and approach their highest levels (top-right corner), their impact becomes more balanced, with the contour lines tilting, indicating a more equal influence. The variation in the calciner cost has a stronger effect on DT-calciner configurations, where the contour lines shift considerably towards lower or higher values depending on the cost variation, while for Ent-calciner processes, this effect is weaker.

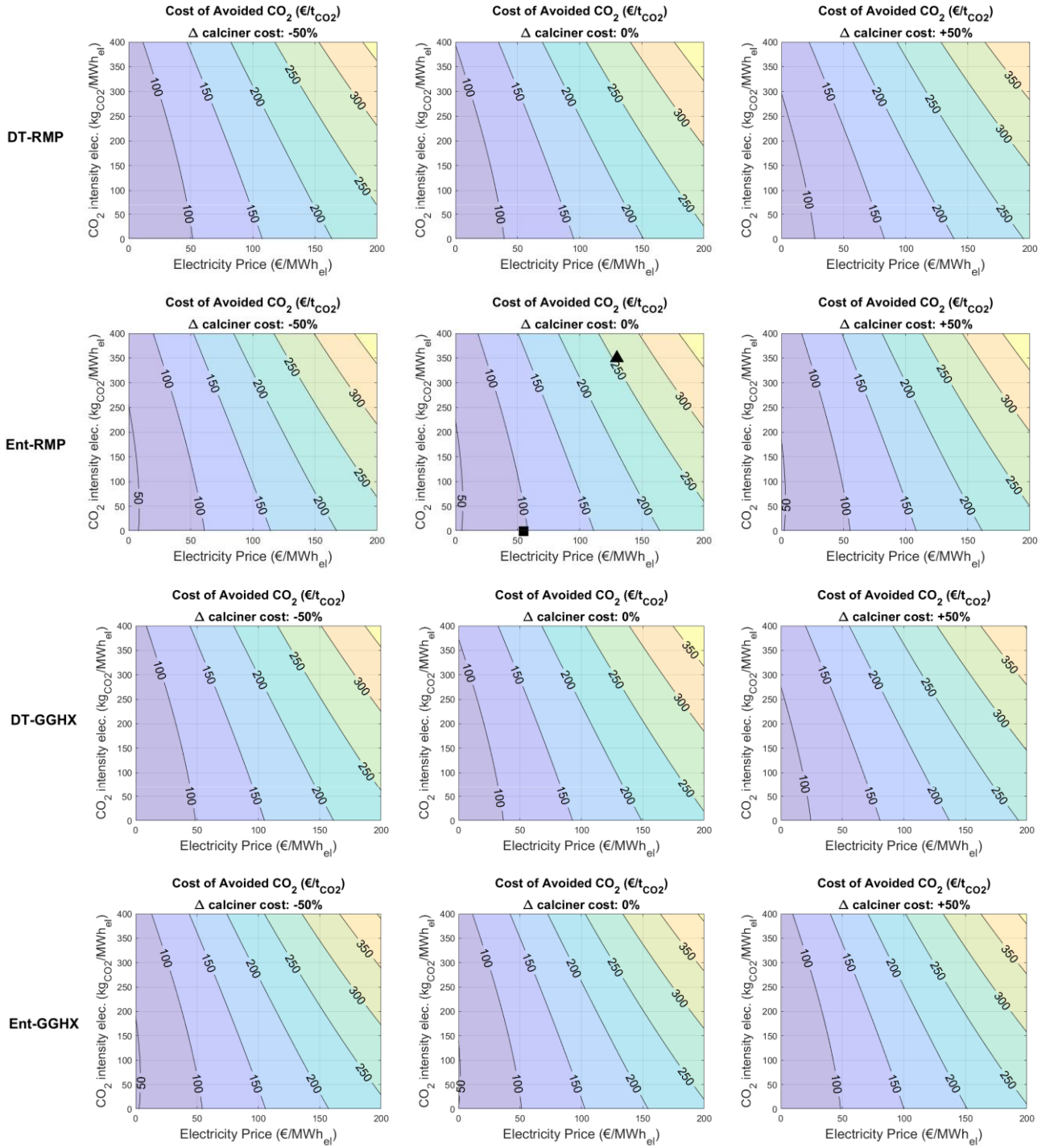


Figure 80. Sensitivity analysis on the cost of avoided CO_2 (CAC) varying electricity price, carbon intensity of electricity and calciner cost simultaneously. DT-RMP = drop tube calciner with pure CO_2 preheating raw meal; Ent-RMP = entrainment calciner with pure CO_2 preheating raw meal; DT-GGHX = drop tube calciner with pure CO_2 preheating vent air via a gas-gas heat exchanger; Ent-GGHX = entrainment calciner with pure CO_2 preheating vent air via a gas-gas heat exchanger. As a matter of example, for Ent-RMP at Δ calciner cost = 0%, we showed how two different energy supply scenarios would position in the plot (■ = solar photovoltaics in the Netherlands; ▲ = natural gas power plant in Germany).

A particularly interesting aspect of these contour plots is their ability to identify combinations of parameters making each configuration economically competitive. For instance, assuming that a carbon capture technology is considered competitive with a CAC lower than 150 €/t CO_2 , the plots

indicate that electricity prices must remain below approximately 90-100 €/MWh_{el} if the electricity is sourced from low-carbon sources and the electrified calciner cost estimate is accurate (0% change).

Should the carbon intensity of electricity rise, or if the actual calciner cost exceeds the estimate, the electricity price would need to decrease further to sustain competitiveness.

From another perspective, the plots offer insights into how different energy supply scenarios affect the economic feasibility of these technologies. By exploring the parameter space in the contour plots, different energy supply scenarios (i.e., combinations of carbon intensity and electricity price) can be represented. Accordingly, the economic feasibility of the technology is demonstrated through the contour lines indicating the *CAC*.

An illustrative example is provided in Figure 10, within the contour plot for the Ent-RMP configuration with a 0% variation in electrified calciner cost. The plot shows that if electricity is supplied from solar photovoltaics (carbon intensity: 0 kgCO_{2,eq}/MWh_{el}) in the Netherlands (levelised cost of electricity: 55 €/MWh_{el}; IRENA, 2024), the technology is competitive, achieving a *CAC* of approximately 97 €/tCO₂. In contrast, using electricity from a modern natural gas power plant (carbon intensity: 350 kgCO_{2,eq}/MWh_{el}; Madejski et al., 2022) built in Germany (levelised cost of electricity: 130 €/MWh_{el}; IRENA, 2024) results in a much higher *CAC* of about 255 €/tCO₂, making the technology less economically attractive. This discussion highlights that access to affordable and low-carbon electricity is crucial for ensuring the cost-effectiveness of these technologies.

While this study provides an insightful preliminary exploration of these aspects, future research should focus on a more detailed and integrated evaluation of the energy system, ideally combining low-carbon technologies that complement those evaluated in this work. One potential approach could be the integration of solid waste incineration technologies, such as municipal or industrial waste. This strategy can further reduce fossil fuel consumption in the rotary kiln or generate low-cost electricity for the electrified calciner, thus supporting the decarbonisation strategies discussed in this study.

Another area for improvement lies in enhancing the energy efficiency of the processes to reduce energy demand, thereby lowering OPEX. This can be achieved by optimising process sections, such

as the amine-based capture, where solvent properties can be tailored to minimise energy consumption based on specific inlet flue gas conditions (Wang et al., 2022).

From a policy perspective, the results underscore that the effective implementation of these technologies in the current European context would require larger carbon emission taxes. In the base case scenario, it was highlighted that this tax should not be lower than 220 €/t_{CO₂} to ensure economic viability. Additionally, offering subsidies for the installation of renewable energy systems within cement factories could further incentivise research and facilitate the transition to electrified technologies, helping to offset initial investment costs and reduce energy-related expenses.

The final analysis examines the effect of uncertainty in the cost estimates for both DT- and Ent-calciners on *CAC* under various electricity price and carbon intensity scenarios (Figure 11). The Ent-calciner cost variation was explored within a range of -50% to +100%, given that the uncertainty surrounding this estimate is significant due to the lack of previous industrial cost assessments.

Conversely, the DT-calciner cost was varied between -50% and +50%, as its cost is already quite high and the estimate is more reliable, being based on an industrial project (LEILAC2, 2023).

The 3D plots of Figure 11 (left-hand side) demonstrate that RMP configurations consistently outperform GGHX configurations, when using the same type of calciner. Additionally, a crossover in *CAC* is observed between the DT-RMP and Ent-RMP, depending on the calciner cost variations. As shown in the right-hand plots, the extent of this crossover can expand or shrink based on the electricity price and carbon intensity considered.

Under base case scenario (Figure 11a), the trade-off between DT-RMP and Ent-RMP occurs when the DT-calciner cost is 30-50% lower than the estimated in this study, while the Ent-calciner cost varies in the range between -15% and +100%. When electricity price decreases to 80 €/MWh_{el} (Figure 11b), Ent-RMP becomes the superior option across nearly the entire range of investigated calciner cost variations. This suggests that lowering electricity prices is more advantageous for Ent-RMP than for DT-RMP.

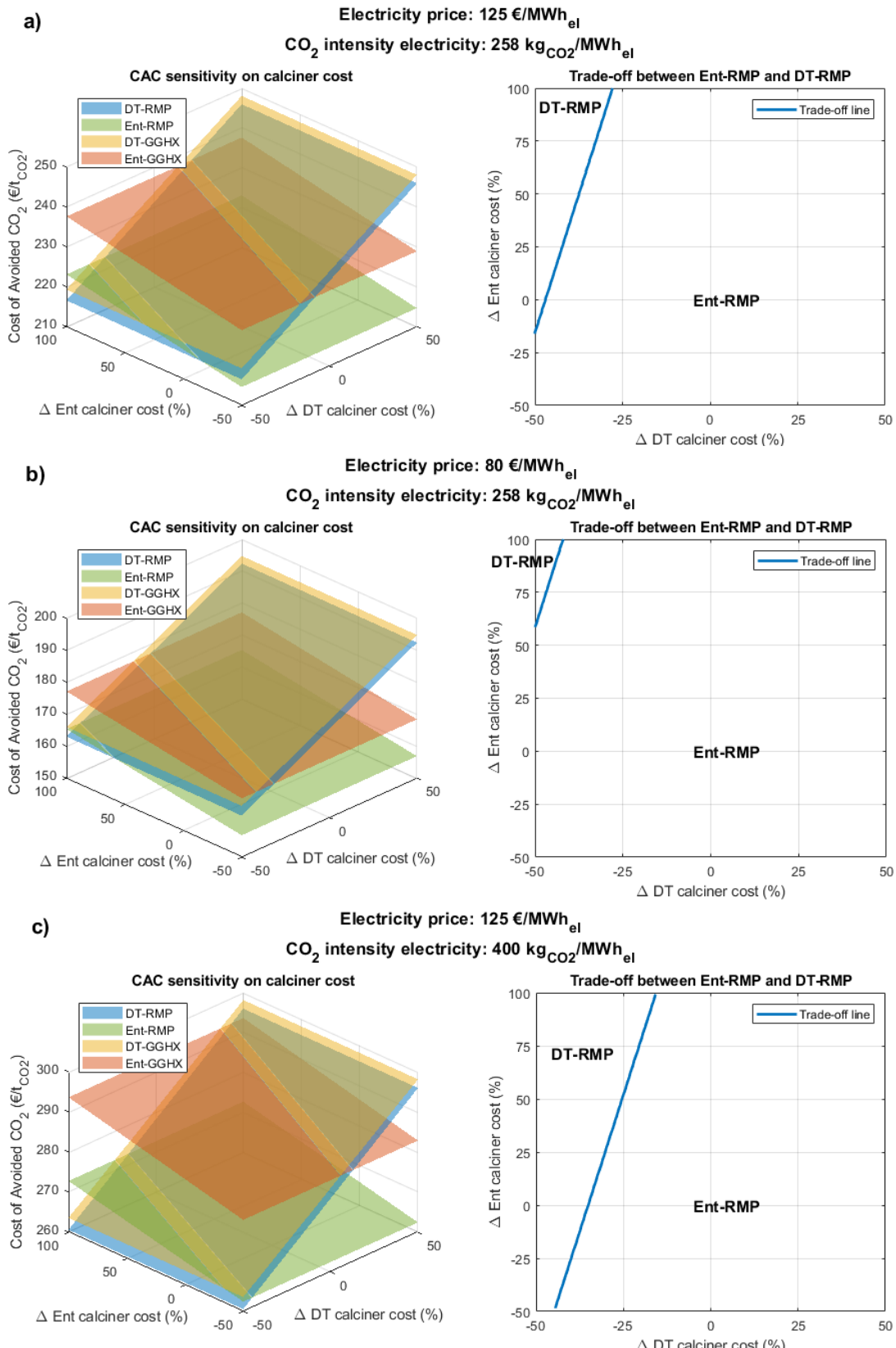


Figure 9. Effect of calciner cost uncertainty on the cost of avoided CO_2 (CAC) and the trade-off between configurations. DT-RMP = drop tube calciner with pure CO_2 preheating raw meal; Ent-RMP = entrainment calciner with pure CO_2 preheating raw meal; DT-GGHX = drop tube calciner with pure CO_2 preheating vent air via a gas-gas heat exchanger; Ent-GGHX = entrainment calciner with pure CO_2 preheating vent air via a gas-gas heat exchanger. The investigation involves different scenarios: (a) electricity price: 125 €/MWh_{el}, carbon intensity electricity: 258 kg_{CO2}/MWh_{el}; (b) electricity price: 80 €/MWh_{el}, carbon intensity electricity: 258 kg_{CO2}/MWh_{el}; (c) electricity price: 125 €/MWh_{el}, carbon intensity electricity: 400 kg_{CO2}/MWh_{el}.

In scenarios where electricity remains very expensive and sourced, for instance, from natural gas (Figure 11c), a broader trade-off emerges between Ent-RMP and DT-RMP. In these cases, the uncertainty in the electrified calciner cost plays a significant role in determining which alternative is more economically favourable. Further research, particularly focused on the electrified calciner design, will be essential to provide clearer expectation regarding the actual performance and cost, thereby increasing the confidence in this technology.

4. Conclusions

This study explored the potential for decarbonising the cement sector by electrifying the calciner and applying amine-based carbon capture on rotary kiln emissions. A techno-economic analysis was conducted on four distinct process alternatives, which differed by the type of calciner used – either entrainment or drop tube, and the heat recovery strategy for the hot CO₂ produced in the electrified calciner.

Low-carbon processes increased electrical energy demand by 5.6 to 6.2 times compared to the reference plant, with entrainment calciner configurations requiring more power due to the energy penalty from CO₂ recycling to lift the solids. All alternatives achieved competitive capture rates of approximately 97.5%, and CO₂ concentrations met the required quality specifications without the need for additional purification. Overall, drop tube calciner designs demonstrated better energy efficiency, achieving comparable capture rates with similar fuel consumption, but lower electrical demand compared to Ent-calciner processes.

Under an EU-27 energy mix, the low-carbon processes reached a CO₂ avoidance rate of 70-72%, which was lower than other promising decarbonisation technologies such as oxyfuel and calcium looping. However, when low-carbon electricity is supplied, the CO₂ avoidance rate improved to 98%, making these processes competitive with both oxyfuel and calcium looping technologies.

From an economic perspective, entrainment calciner with raw materials preheating emerged as the most favourable configuration with a cost of clinker (*COC*) of 213.4 €/t_{clk} and a cost of avoided CO₂ (*CAC*) of 217.4 €/t_{CO2}, primarily due to the lower CAPEX of the electrified calciner and amine capture system. The other scenarios showed comparable economic performance, with *CAC* values between 231-234 €/t_{CO2}. The high *CAC* values observed in the baseline scenario revealed that these technologies are not yet economically viable, mainly due to the current electricity price in the EU. A sensitivity analysis through a response surface model highlighted that the competitiveness of low-carbon cement plants is strongly influenced by electricity price and grid carbon intensity. Further research focusing on detailed calciner design, accurate cost estimation, and the optimisation of processes and energy systems is critical to enabling widespread adoption and ensuring economic viability.

CRediT authorship contribution statement

Leonardo Varnier: Conceptualisation, Formal analysis, Investigation, Methodology, Software, Visualisation, Writing – original draft. **Federico d'Amore:** Methodology, Supervision, Validation, Writing – review and editing. **Kim Clausen:** Methodology, Supervision, Validation, Writing – review and editing. **Georgios Melitos:** Methodology, Software, Writing – review and editing. **Bart de Groot:** Software, Writing – review and editing. **Fabrizio Bezzo:** Methodology, Supervision, Writing – review and editing, Funding acquisition.

Declaration of competing interest

The authors declare the following financial interests/personal relationships which may be considered as potential competing interests: K.C. is an employee of FLSmidth Cement A/S and G.M and B.d.G are employees of Siemens Industry Software Limited.

Data availability

Data will be made available on request.

Acknowledgements

This work has been funded by the European Union's Horizon Europe research and innovation programme under the Marie Skłodowska-Curie Grant Agreement No 101073547 "CO2Valorize".

FdA acknowledges of the support of the National Recovery and Resilience Plan (NRRP), Mission 4 Component 2 Investment 1.4 - Call for tender No. 3138 of December 16, 2021 of the Italian Ministry of University and Research, funded by the European Union - NextGenerationEU [Award Number: CNMS named MOST, Concession Decree No. 1033 of June 17, 2022, adopted by the Italian Ministry of University and Research, CUP: C93C22002750006, Spoke 14 "Hydrogen and New Fuels"].

Nomenclature

Acronyms

BAT	Best Available Technique
BF	Bag Filter
CAPEX	Capital cost
CCS	Carbon capture and storage
COP	Coefficient of performance
CPU	Compression and Purification Unit
DT	Drop tube
ESP	Electrostatic precipitator
Ent	Entrainment
GGHX	Gas-gas heat exchanger configuration
KPIs	Key performance indicators
LHV	Lower heating value
MEA	Monoethanolamine
PCC	Post-combustion carbon capture
RMP	Raw meal preheating configuration
SNCR	Selective non-catalytic reduction

Symbols

AC_{eq}	%	Equivalent CO ₂ avoided
BEC	€	Bare erected cost
CAC	€/t _{CO₂}	Cost of avoided CO ₂
CCR	%	Carbon capture rate
c_{CO_2}	€/t _{CO₂}	Carbon tax

c_{el}	€/MWh _{el}	Electricity cost (with carbon tax)
$c_{el,base}$	€/MWh _{el}	Base cost of electricity (without carbon tax)
COC	€/t _{clk}	Cost of clinker
EC	€	Equipment cost
$e_{capt,clk}$	kg _{CO₂} /t _{clk}	Specific CO ₂ captured
e_{clk}	kg _{CO₂} /t _{clk}	Direct specific CO ₂ emissions
e_{el}	kg _{CO_{2,eq}} /MWh _{el}	Carbon intensity of the imported electricity
$e_{el,clk}$	kg _{CO₂} /t _{clk}	Equivalent specific CO ₂ emissions
$e_{eq,clk}$	kg _{CO₂} /t _{clk}	Equivalent specific CO ₂ emissions
i	%	Discount rate
IF	—	Installation factor
j	—	Generic unit
\dot{m}_{clk}	[t _{clk} /y]	Annual clinker productivity
ML	€/y	Maintenance labour cost
n	y	Plant operational life
OL	€/y	Operating labour cost
$OPEX$	€/y	Operative costs
$P_{el,clk}$	MWh _{el} /t _{clk}	Electrical energy consumption
TAC	€/y	Total annualised CAPEX
TDC	€	Total direct cost
TOC	€	Total overnight cost
TPC	€	Total plant cost

Sub-/Superscripts

clk Clinker

decarb	Plant with decarbonisation measure
el	Electric
eq	Equivalent
ref	Reference unabated plant
th	Thermal

References

AC2OCEM. (2019). *Accelerating Carbon Capture Using Oxyfuel Technology in Cement Production*.
<https://ac2ocem.eu-projects.de/> (accessed 6 September 2024)

Anantharaman, R., Berstad, D., Cinti, G., De Lena, E., Gatti, M., Gazzani, M., Hoppe, H., Martínez, I., Garcia Moretz-Sohn Monteiro, J., Romano, M., Roussanaly, S. E., Schols, E., Spinelli, M., Størset, S., van Os, P., and Voldsgaard, M. (2017). *CEMCAP framework for comparative techno-economic analysis of CO₂ capture from cement plants*. *CEMCAP Deliverable D3.2*.
<https://zenodo.org/records/1257112#.W8hidapPpaR> (accessed 16 October 2024)

Antunes, M., Santos, R. L., Pereira, J., Rocha, P., Horta, R. B., and Colaço, R. (2022). Alternative clinker technologies for reducing carbon emissions in cement industry: A critical review. *Materials*, 15(1), 209. <https://doi.org/10.3390/ma15010209>

Arpagaus, C., Bless, F., Uhlmann, M., Schiffmann, J., and Bertsch, S. S. (2018). High temperature heat pumps: Market overview, state of the art, research status, refrigerants, and application potentials. *Energy*, 152, 985–1010. <https://doi.org/10.1016/j.energy.2018.03.166>

Bonnickson, K. R. (1954). Heat Contents of Calcium and Magnesium Ferrites. *Journal of the American Chemical Society*, 76(6), 1480–1482. <https://doi.org/10.1021/ja01635a006>

Bonnickson, K. R. (1955). High Temperature Heat Contents of Aluminates of Calcium and Magnesium. *The Journal of Physical Chemistry*, 59(3), 220–221.
<https://doi.org/10.1021/j150525a006>

Campanari, S., Cinti, G., Consonni, S., Fleiger, K., Gatti, M., Hoppe, H., Martínez, I., Romano, M., Spinelli, M., & Voldsgaard, M. (2016). *Design and performance of CEMCAP cement plant without CO₂ capture*. *CEMCAP Deliverable D4.1*.
<https://zenodo.org/records/1001664#.WnQkZmfrtaQ> (accessed 2 September 2024)

Catch4Climate. (2020). *Catch4Climate project*. <https://database.co2value.eu/projects/209> (accessed 6 September 2024)

Cavalett, O., Watanabe, M. D. B., Voldsgaard, M., Roussanaly, S., and Cherubini, F. (2024). Paving the way for sustainable decarbonization of the European cement industry. *Nature Sustainability*, 7, 568–580. <https://doi.org/10.1038/s41893-024-01320-y>

CEMCAP. (2015). *EU H2020 Project: CO₂ Capture from Cement Production*. <https://doi.org/10.3030/641185> (accessed 18 September 2024)

Chemical Engineering. (2024). *Chemical Engineering Plant Cost Index (CEPCI)*. <https://www.chemengonline.com/site/plant-cost-index/> (accessed 4 November 2024)

Cinti, G., Anantharaman, R., De Lena, E., Fu, C., Gardarsdottir, S. O., Hoppe, H., Jamali, A., Romani, M., Roussanaly, S., Spinelli, M., Stallmann, O., and Voldsgaard, M. (2018). *Cost of critical components in CO₂ capture processes. CEMCAP Deliverable D4.4*. <https://zenodo.org/records/2593219#.XJoyDPZFzeQ> (accessed 8 September 2024)

CLEANER. (2017). *EU H2020 Project: CLEAN clinKER production by Calcium looping process*. <https://doi.org/10.3030/764816> (accessed 3 October 2024)

Cormos, C. C. (2022). Decarbonization options for cement production process: A techno-economic and environmental evaluation. *Fuel*, 320, 123907. <https://doi.org/10.1016/j.fuel.2022.123907>

d'Amore, F., Nava, A., Colbertaldo, P., Visconti, C. G., and Romano, M. C. (2023). Turning CO₂ fuel combustion into e-Fuel? Consider alternative pathways. *Energy Conversion and Management*, 289, 117170. <https://doi.org/10.1016/j.enconman.2023.117170>

d'Amore, F., Romano, M. C., and Bezzo, F. (2021). Optimal design of European supply chains for carbon capture and storage from industrial emission sources including pipe and ship transport. *International Journal of Greenhouse Gas Control*, 109, 103372. <https://doi.org/10.1016/j.ijggc.2021.103372>

De Lena, E., Spinelli, M., Gatti, M., Scaccabarozzi, R., Campanari, S., Consonni, S., Cinti, G., and Romano, M. C. (2019). Techno-economic analysis of calcium looping processes for low CO₂ emission cement plants. *International Journal of Greenhouse Gas Control*, 82, 244–260. <https://doi.org/10.1016/j.ijggc.2019.01.005>

EEA. (2024). *Greenhouse gas emission intensity of electricity generation*. <https://www.eea.europa.eu/en/analysis/indicators/greenhouse-gas-emission-intensity-of-1> (accessed 9 October 2024)

Ember. (2024). *European electricity prices and costs - Electricity and carbon prices*. <https://ember-climate.org/data/data-tools/european-electricity-prices-and-costs/> (accessed 7 September 2024)

Eurostat. (2024). *Electricity prices for non-household consumers - bi-annual data (from 2007 onwards)*. https://doi.org/https://doi.org/10.2908/NRG_PC_205 (accessed 15 September 2024)

Gardarsdottir, S. O., De Lena, E., Romano, M., Roussanaly, S., Voldsgaard, M., Pérez-Calvo, J. F., Berstad, D., Fu, C., Anantharaman, R., Sutter, D., Gazzani, M., Mazzotti, M., and Cinti, G. (2019). Comparison of technologies for CO₂ capture from cement production—Part 2: Cost analysis. *Energies*, 12(3), 542. <https://doi.org/10.3390/en12030542>

GCCA. (2021). *Concrete Future - The GCCA 2050 Cement and Concrete Industry Roadmap for Net Zero Concrete*. <https://gccaassociation.org/concretefuture/wp-content/uploads/2022/10/GCCA-Concrete-Future-Roadmap-Document-AW-2022.pdf> (accessed 2 September 2024)

Haas, J. L., Robinson, G. R., and Hemingway, B. S. (1981). Thermodynamic tabulations for selected phases in the system CaO-Al₂O₃-SiO₂-H₂O at 101.325 kPa (1 atm) between 273.15 and 1800 K. *Journal of Physical and Chemical Reference Data*, 10(3), 575–670. <https://doi.org/10.1063/1.555645>

Hanein, T., Glasser, F. P., and Bannerman, M. N. (2020). Thermodynamic data for cement clinkering. *Cement and Concrete Research*, 132, 106043. <https://doi.org/10.1016/j.cemconres.2020.106043>

Hewlett, P. C., & Liska, M. (2019). *Lea's Chemistry of Cement and Concrete* (5th ed.). Butterworth-Heinemann. <https://doi.org/10.1016/C2013-0-19325-7>

Hills, T., Leeson, D., Florin, N., and Fennell, P. (2016). Carbon Capture in the Cement Industry: Technologies, Progress, and Retrofitting. *Environmental Science and Technology*, 50(1), 368–377. <https://doi.org/10.1021/acs.est.5b03508>

IEA. (2018). *Technology Roadmap - Low-Carbon Transition in the Cement Industry*. <https://www.iea.org/reports/technology-roadmap-low-carbon-transition-in-the-cement-industry> (accessed 2 September 2024)

IEA. (2019). *CO₂ Emissions from Fuel Combustion 2019*. OECD. <https://doi.org/10.1787/2a701673-en> (accessed 13 September 2024)

IEAGHG. (2013). *Deployment of CCS in the Cement Industry*. <https://ieaghg.org/publications/deployment-of-ccs-in-the-cement-industry/> (accessed 6 September 2024)

IRENA. (2024). *Renewable power generation costs in 2023*. https://www.irena.org/-/media/Files/IRENA/Agency/Publication/2024/Sep/IRENA_Renewable_power_generation_costs_in_2023.pdf (accessed 17 January 2025)

Jacob, R. M., Pinheiro, J. P., and Tokheim, L. A. (2023). Electrified externally heated rotary calciner for calcination of cement raw meal. *Heliyon*, 9(11), e22023. <https://doi.org/10.1016/j.heliyon.2023.e22023>

Jacob, R. M., and Tokheim, L. A. (2023). Electrified calciner concept for CO₂ capture in pyro-processing of a dry process cement plant. *Energy*, 268, 126673. <https://doi.org/10.1016/j.energy.2023.126673>

Jacob, R. M., and Tokheim, L.-A. (2021). Electrification of an Entrainment Calciner in a Cement Kiln System – Heat Transfer Modelling and Simulations. *Proceedings of 62nd SIMS, September 21-23, Virtual Conference*, 185, 67–75. <https://doi.org/10.3384/ecp2118567>

LEILAC. (2016). *EU H2020 project: Low Emissions Intensity Lime and Cement*. <https://doi.org/10.3030/654465> (accessed 9 September 2024)

LEILAC2. (2020). *EU H2020 project: Low Emissions Intensity Lime and Cement 2: Demonstration Scale*. <https://doi.org/10.3030/884170> (accessed 14 September 2024)

LEILAC2. (2023). *A techno-economic analysis of the Leilac technology at full commercial scale*. <https://www.leilac.com/wp-content/uploads/2023/10/2023-10-15-Techno-Economic-Analysis->

of-Leilac-Technology-at-Full-Commercial-Scale-EC-Deliverable-PDF-Version.pdf (accessed 8 September 2024)

Linstrom, P. J., and Mallard, W. G. (2001). The NIST Chemistry WebBook: A chemical data resource on the Internet. *Journal of Chemical and Engineering Data*, 46(5), 1059–1063. <https://doi.org/10.1021/je000236i>

Madeddu, S., Ueckerdt, F., Pehl, M., Peterseim, J., Lord, M., Kumar, K. A., Krüger, C., and Luderer, G. (2020). The CO₂ reduction potential for the European industry via direct electrification of heat supply (power-to-heat). *Environmental Research Letters*, 15(12), 124004. <https://doi.org/10.1088/1748-9326/abbd02>

Madejski, P., Chmiel, K., Subramanian, N., and Kuś, T. (2022). Methods and Techniques for CO₂ Capture: Review of Potential Solutions and Applications in Modern Energy Technologies. *Energies*, 15(3), 887. <https://doi.org/10.3390/en15030887>

Magli, F., Spinelli, M., Fantini, M., Romano, M. C., and Gatti, M. (2022). Techno-economic optimization and off-design analysis of CO₂ purification units for cement plants with oxyfuel-based CO₂ capture. *International Journal of Greenhouse Gas Control*, 115, 103591. <https://doi.org/10.1016/j.ijggc.2022.103591>

Manzolini, G., Sanchez Fernandez, E., Rezvani, S., Macchi, E., Goetheer, E. L. V., and Vlugt, T. J. H. (2015). Economic assessment of novel amine based CO₂ capture technologies integrated in power plants based on European Benchmarking Task Force methodology. *Applied Energy*, 138, 546–558. <https://doi.org/10.1016/j.apenergy.2014.04.066>

Marmier, A. (2023). *Decarbonisation options for the cement industry*. <https://doi.org/10.2760/174037> (accessed 10 October 2024)

Mastropasqua, L., Pierangelo, L., Spinelli, M., Romano, M. C., Campanari, S., and Consonni, S. (2019). Molten Carbonate Fuel Cells retrofits for CO₂ capture and enhanced energy production in the steel industry. *International Journal of Greenhouse Gas Control*, 88, 195–208. <https://doi.org/10.1016/j.ijggc.2019.05.033>

Mcbride, B. J., Zehe, M. J., and Gordon, S. (2002). *NASA Glenn Coefficients for Calculating Thermodynamic Properties of Individual Species*. <https://ntrs.nasa.gov/citations/20020085330> (accessed 14 April 2024)

Miller, S. A., Horvath, A., and Monteiro, P. J. M. (2016). Readily implementable techniques can cut annual CO₂ emissions from the production of concrete by over 20%. *Environmental Research Letters*, 11(7), 074029. <https://doi.org/10.1088/1748-9326/11/7/074029>

NETL. (2019). *Capital Cost Scaling Methodology: Revision 4 Report*. <https://doi.org/10.2172/1573493> (accessed 11 October 2024)

Nhuchhen, D. R., Sit, S. P., and Layzell, D. B. (2021). Alternative fuels co-fired with natural gas in the pre-calciner of a cement plant: Energy and material flows. *Fuel*, 295, 120544. <https://doi.org/10.1016/j.fuel.2021.120544>

Plaza, M. G., Martínez, S., and Rubiera, F. (2020). CO₂ capture, use, and storage in the cement industry: State of the art and expectations. *Energies*, 13(21), 5692. <https://doi.org/10.3390/en13215692>

Quevedo Parra, S., and Romano, M. C. (2023). Decarbonization of cement production by electrification. *Journal of Cleaner Production*, 425, 138913. <https://doi.org/10.1016/j.jclepro.2023.138913>

Rubin, E. S., Short, C., Booras, G., Davison, J., Ekstrom, C., Matuszewski, M., and McCoy, S. (2013). A proposed methodology for CO₂ capture and storage cost estimates. *International Journal of Greenhouse Gas Control*, 17, 488–503. <https://doi.org/10.1016/j.ijggc.2013.06.004>

Sanchez Fernandez, E., Goetheer, E. L. V., Manzolini, G., Macchi, E., Rezvani, S., and Vlugt, T. J. H. (2014). Thermodynamic assessment of amine based CO₂ capture technologies in power plants based on European Benchmarking Task Force methodology. *Fuel*, 129, 318–329. <https://doi.org/10.1016/j.fuel.2014.03.042>

Schneider, M., Hoenig, V., Ruppert, J., and Rickert, J. (2023). The cement plant of tomorrow. *Cement and Concrete Research*, 173, 107290. <https://doi.org/10.1016/j.cemconres.2023.107290>

Schorcht, F., Kourtzi, I., Scalet, B. M., Roudier, S., and Delgado Sancho, L. (2013). *Best Available Techniques (BAT) Reference for the production of cement Lime and Magnesium Oxide*. https://eippcb.jrc.ec.europa.eu/sites/default/files/2019-11/CLM_Published_def_0.pdf (accessed 20 September 2024)

Siemens. (2024). *gPROMS Process* Version 2023.2.0. <https://www.siemens.com/global/en/products/automation/industry-software/gproms-digital-process-design-and-operations/gproms-modelling-environments/gproms-process.html> (accessed 1 October 2024)

Strunge, T., Küng, L., Sunny, N., Shah, N., Renforth, P., and Van der Spek, M. (2024). Finding least-cost net-zero CO₂e strategies for the European cement industry using geospatial techno-economic modelling. *RSC Sustainability*, 2, 3054–3076. <https://doi.org/10.1039/D4SU00373J>

Tokheim, L.-A., Mathisen, A., Øi, L. E., Jayarathna, C., Eldrup, N., and Gautestad, T. (2019). Combined calcination and CO₂ capture in cement clinker production by use of electrical energy.

Proceedings of TCCS-10, June 17-19, 101–109. <https://www.researchgate.net/publication/338553982> (accessed 3 September 2024)

van der Spek, M., Roussanaly, S., and Rubin, E. S. (2019). Best practices and recent advances in CCS cost engineering and economic analysis. *International Journal of Greenhouse Gas Control*, 83, 91–104. <https://doi.org/10.1016/j.ijggc.2019.02.006>

Turton, R., Shaeiwitz, J. A., Bhattacharyya, D., & Whiting, W. B. (2018). *Analysis, Synthesis, and Design of Chemical Processes* (5th ed.). Prentice Hall.

Voldsdund, M., Gardarsdottir, S. O., De Lena, E., Pérez-Calvo, J. F., Jamali, A., Berstad, D., Fu, C., Romano, M., Roussanaly, S., Anantharaman, R., Hoppe, H., Sutter, D., Mazzotti, M., Gazzani, M., Cinti, G., and Jordal, K. (2019). Comparison of technologies for CO₂ capture from cement production—Part 1: Technical evaluation. *Energies*, 12(3), 559. <https://doi.org/10.3390/en12030559>

Wagner, W., and Pruß, A. (2002). The IAPWS formulation 1995 for the thermodynamic properties of ordinary water substance for general and scientific use. *Journal of Physical and Chemical Reference Data*, 31(2), 387–535. <https://doi.org/10.1063/1.1461829>

Wang, Y., Guo, L., Wang, B. and Klemeš, J. J., A graphical approach for mixed ratio optimisation in the binary mixed amine solution, *Journal of Environmental Management*, Volume 311, 2022, 114779

Wang, Y., Guo, L., Wang, B., and Klemeš, J. J. (2022). A graphical approach for mixed ratio optimisation in the binary mixed amine solution. *Journal of Environmental Management*, 311. <https://doi.org/10.1016/j.jenvman.2022.114779>

Wilhelmsen, B., Kollberg, C., Larsson, J., Eriksson, J., and Eriksson, M. (2018). *CemZero. A feasibility study evaluating ways to reach sustainable cement production via the use of electricity.*

https://www.cement.heidelbergmaterials.se/sites/default/files/assets/document/65/de/final_cemzero_2018_public_version_2.0.pdf.pdf (accessed 6 September 2024)

Yang, F., Meerman, J. C., and Faaij, A. P. C. (2021). Carbon capture and biomass in industry: A techno-economic analysis and comparison of negative emission options. *Renewable and Sustainable Energy Reviews*, 144, 111028. <https://doi.org/10.1016/j.rser.2021.111028>